Meson exchange currents in electromagnetic one-nucleon emission

Carlotta Giusti and Franco Davide Pacati
Dipartimento di Fisica Nucleare e Teorica, Università di Pavia
and Istituto Nazionale di Fisica Nucleare, Sezione di Pavia, I-27100 Pavia, Italy
(Received 4 November 2002; published 2 April 2003)

The role of meson exchange currents (MEC) in electron- and photon-induced one-nucleon emission processes is studied in a nonrelativistic model including correlations and final state interactions. The nuclear current is the sum of a one-body and of a two-body part. The two-body current includes pion seagull, pion-in-flight, and the isobar current contributions. Numerical results are presented for the exclusive ^{16}O$(e,e'p)^{15}$N and ^{16}O$(\gamma,p)^{15}$N reactions. MEC effects are in general rather small in $(e,e'p)$, while in (γ,p) they are always large and important to obtain a consistent description of $(e,e'p)$ and (γ,p) data, with the same spectroscopic factors. The calculated (γ,p) cross sections are sensitive to short-range correlations at high values of the recoil momentum, where MEC effects are larger and overwhelm the contribution of correlations.

DOI: 10.1103/PhysRevC.67.044601 PACS number(s): 25.20.Lj, 25.30.Fj, 24.10.Eq

I. INTRODUCTION

Electromagnetic knockout reactions with one-nucleon emission have provided in the last decades a wealth of information on the single particle (sp) properties of light, medium, and heavy nuclei [1–4]. The electromagnetic probe is particularly well suited for studying the nuclear properties as its relatively weak interaction with the nuclear matter allows to penetrate deeply in the nucleus interior and to explore also the inner states.

The distorted wave impulse approximation (DWIA) has successfully been applied to the analysis of experimental data produced by these reactions. The overlap integral between the target bound state and the different states of the residual nucleus, which can be obtained from a one-body potential able to reproduce the binding energy and the density of the sp states, was found in agreement with the many-body mean-field calculations. Moreover, an optical potential derived from elastic nucleon scattering off nuclei was able to well reproduce the shape of the reduced cross sections, which are essentially the distorted momentum distributions of nucleons in the nucleus. This means that the gross features of the reaction are well understood.

Many particular aspects of the reaction mechanism have been studied, such as relativistic corrections of the nuclear current and off-shell effects due to the binding of the initial nucleon in the nuclear medium. Moreover, the Coulomb distortion of the incoming and outgoing electron waves in the electron field of the nucleus was studied [5] and also an exact treatment was applied, which calculates the solutions of the Dirac equations for the partial waves [6,7]. More recently, complete relativistic calculations [8,9] have been compared with the new data at higher energy obtained at TJNAF [10].

Despite these interesting results, some problems are still open and have found only a partial solution. The low value of the spectroscopic factors, which are about 60–70 % of the values predicted by the independent-particle shell model, addresses to more complicate mechanisms than the one-body one in the frame of a mean-field theory. Moreover, consistency between electron- and photon-induced reactions is required and should be obtained in the same theory frame. Strong difficulties, on the contrary, have to be faced when treating, in particular, the reactions with neutron emission. In addition, the study of higher energy processes has shown up ambiguities in the choice of the nuclear current operator [9], which must be eliminated in a consistent theory.

Different mechanisms have been advocated in order to solve these problems. First of all, nucleon-nucleon correlations, which produce the defect in the spectroscopic factors of the hole spectral functions. Theoretical investigations with different correlation methods [11–16] indicate that only a few percent of the defect is due to short-range correlations (SRC). When tensor correlations are added the depletion amounts to $\sim$10%, at most $\sim$15% in heavy nuclei. Further depletion is given by long-range correlations [17–20]. A full and consistent evaluation of all the different types of correlations, which affect the spectroscopic factors and the overlap functions to be included in the DWIA approach, is anyhow still unavailable.

Multistep processes have also been considered in the treatment of the final state interaction of knockout reactions, but they were shown to give a sizable contribution only at high excitation energy or missing momenta [21].

In this paper, we discuss the effect of two-body meson exchange currents (MEC) both in $(e,e'p)$ and in (γ,p) reactions. This topic has already been discussed in some papers with different approaches [23–29]. Some disagreements are present in the results of the various groups. In general, the effects were found significant, but large only in the region of high recoil momenta. Moreover, in the $(e,e'p)$ reaction the response functions appear more sensitive to MEC effects than the total cross sections. It is not surprising that some differences can be found between the results of the different models, even when the operators describing MEC are identical, due to interference between the different ingredients of the calculations. A further study seems, therefore, useful to clarify the situation.

In this work MEC effects are evaluated in the frame of a nonrelativistic direct knockout (DKO) model with final state interactions. The direct one-body contribution corresponds to the DWIA approach, which was successfully applied to the analysis of $(e,e'p)$ data at moderate energy [3,22]. The interaction occurs in the initial state through a one-body and a two-body current with a pair of nucleons. Only one nucleon is emitted and the other one is reabsorbed in the residual nucleus. Correlations can be directly included in the sp wave functions or with a central correlation function. This approach was originally proposed in Ref. [24] and has more recently been applied to the (γ,p) reaction [16,30] and, in a relativistic model, to the $(e,e'p)$ and (γ,p) reactions [32]. In these previous applications, however, only the pion-seagull term was included in the two-body current. Moreover, in Refs. [16,24,30] a simplified treatment of the spin was used in order to reduce the complexity of the numerical calculations, and the spin-orbit term was neglected in the optical potential.

A more refined theoretical model is considered in this paper. The two-body current includes the contribution of all the diagrams with one-pion exchange, namely, seagull, pion-in-flight, and the diagrams with intermediate Δ-isobar configurations. Moreover, also spin coupling and the spin-orbit term of the optical potential are fully included in the calculations. Application of this model to the $(e,e'p)$ and (γ,p) reactions and comparison with data allow us to check the consistency of the description of electron- and photon-induced reactions within the same theoretical framework.

In Sec. II, the relevant formalism and the parameters used in the calculation are given. Numerical results are presented and discussed in Sec. III for the cross section and the structure functions of the exclusive $^{16}\mathrm{O}(e,e'p)^{15}\mathrm{N}$ reaction and for the cross section of the exclusive $^{16}\mathrm{O}(\gamma,p)^{15}\mathrm{N}$ reaction. Some conclusions are drawn in Sec. IV.

II. THEORETICAL MODEL

The coincidence unpolarized cross section for the reaction induced by an electron, with momentum $\boldsymbol{p}_0$ and energy E_0, with $E_0=|\boldsymbol{p}_0|=p_0$, where a nucleon, with momentum $\boldsymbol{p}'$ and energy E', is ejected from a nucleus, is given, in the one-photon exchange approximation and after integrating over the energy of the emitted nucleon, by [3]

$$\frac{d^5\sigma}{dE_0'd\Omega_0'd\Omega'}=K[2\epsilon_{\mathrm{L}}f_{00}+f_{11}-\epsilon f_{1-1}\cos 2\alpha + \sqrt{\epsilon_{\mathrm{L}}(1+\epsilon)}f_{01}\cos\alpha]. \tag{1}$$

Here E_0' is the energy of the scattered electron, α is the angle between the plane of the electrons and the plane containing the momentum transfer $\boldsymbol{q}$ and $\boldsymbol{p}'$. The quantity

$$\epsilon=\left(1-\frac{2\boldsymbol{q}^2}{q_\nu^2}\tan^2\frac{\theta}{2}\right)^{-1} \tag{2}$$

measures the polarization of the virtual photon exchanged by the electron scattered at an angle θ and

$$\epsilon_{\mathrm{L}}=-\frac{q_\nu^2}{\boldsymbol{q}^2}\epsilon, \tag{3}$$

where $q_\mu^2=\omega^2-\boldsymbol{q}^2$ with $\omega=p_0-p_0'$ and $\boldsymbol{q}=\boldsymbol{p}_0-\boldsymbol{p}_0'$, is the four-momentum transfer. The coefficient

$$K=\frac{e^4}{16\pi^2}\frac{\Omega_{\mathrm{f}}}{f_{\mathrm{R}}}\frac{E_0'}{E_0 q_\nu^2(\epsilon-1)}, \tag{4}$$

contains the phase-space factor $\Omega_{\mathrm{f}}=p'E'$ and the recoil factor f_{R}^{-1}, with

$$f_{\mathrm{R}}=1+\frac{E'}{E_{\mathrm{B}}}\left(1-\frac{q}{p'}\cos\gamma\right), \tag{5}$$

where E_{B} is the total relativistic energy of the residual nucleus and γ is the angle between $\boldsymbol{q}$ and $\boldsymbol{p}'$.

The structure functions $f_{\lambda\lambda'}$ represent the response of the nucleus to the longitudinal $(\lambda=0)$ and transverse $(\lambda=\pm 1)$ components of the electromagnetic interaction and only depend on ω, q, p', and γ. In Eq. (1) current conservation and gauge invariance have been exploited in order to express the third components of the current, including both one-body and two-body parts, and of the electromagnetic potential in terms of the charge component and the scalar potential, respectively.

When the nucleon is emitted by a real unpolarized photon, only f_{11} contributes. Then, the cross section of the (γ,N) reaction reads

$$\frac{d^2\sigma}{d\Omega'}=\frac{\pi e^2}{2E_\gamma}\frac{\Omega_{\mathrm{f}}}{f_{\mathrm{R}}}f_{11}, \tag{6}$$

where E_γ is the energy of the incident photon.

The structure functions are given in terms of the hadron tensor [3]

$$W^{\mu\nu}=\overline{\sum_{\mathrm{i}}}\sum_{\mathrm{f}} J^\mu(\boldsymbol{q})J^{\nu *}(\boldsymbol{q})\,\delta(E_{\mathrm{i}}-E_{\mathrm{f}}). \tag{7}$$

The quantities $J^\mu(\boldsymbol{q})$ are the Fourier transforms of the transition matrix elements of the nuclear charge-current density operator between initial and final nuclear states

$$J^\mu(\boldsymbol{q})=\int\langle\Psi_{\mathrm{f}}|\hat{J}^\mu(\boldsymbol{r})|\Psi_{\mathrm{i}}\rangle \mathrm{e}^{\mathrm{i}\boldsymbol{q}\cdot\boldsymbol{r}}d\boldsymbol{r}. \tag{8}$$

The nuclear current operator is given in terms of one-body and two-body components. It can be written in the coordinate representation as

$$\hat{J}^\mu(\boldsymbol{r})=\sum_{i=1}^{A}J^{(1)\mu}(\boldsymbol{r},\boldsymbol{r}_i)+\sum_{i<j=1}^{A}J^{(2)\mu}(\boldsymbol{r},\boldsymbol{r}_i,\boldsymbol{r}_j), \tag{9}$$

where the spin and isospin indices are omitted for simplicity.

With the one-body current we have a direct and an exchange contribution. The real or virtual photon hits one nucleon which can be directly emitted (direct process), or can interact with another nucleon through a correlation and then this second nucleon of the pair is emitted (exchange process). A two-body mechanism acts with the two-body cur-

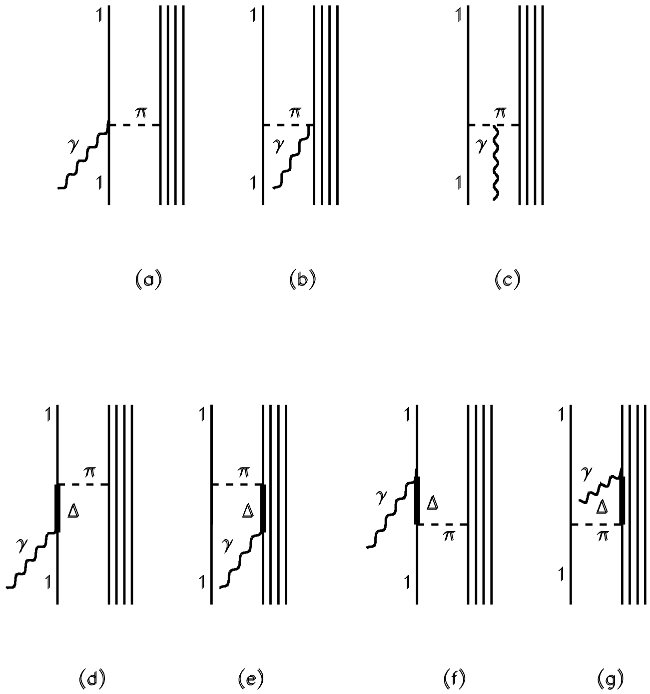

FIG. 1. The two-body exchange current produced by pion exchange. (a) and (b) the contact or seagull current, (c) the pion-in-flight current. (d) and (e) depict the Δ-isobar excitation, (f) and (g) the Δ-isobar deexcitation current.

rent, where the photon is absorbed involving a meson exchange between a pair of nucleons: one of them is emitted and the other one is reabsorbed in the residual nucleus. Thus, the interaction occurs only on a nucleon pair, while the other A-2 nucleons behave as spectators. For the nucleon that is not emitted in the pair, however, a sum over all the sp states in the shell model is performed, and all these states are assumed to be fully occupied.

Taking into account the antisymmetrization of the initial and final nuclear state and including a correlation function of Jastrow type $f(r_{ij})$, with $r_{ij}=|\boldsymbol{r}_i-\boldsymbol{r}_j|$, the current matrix element can be written as

$$\langle\Psi_{\mathrm{f}}|J^{\mu}|\Psi_{\mathrm{i}}\rangle\simeq\sum_{\alpha=1}^{\mathrm{A}}\langle\chi^{(-)}(\boldsymbol{r}_1)\varphi_{\alpha}(\boldsymbol{r}_2)|j^{\mu}(\boldsymbol{r},\boldsymbol{r}_1,\boldsymbol{r}_2)|f(r_{12})\times[\varphi_{\beta}(\boldsymbol{r}_1)\varphi_{\alpha}(\boldsymbol{r}_2)-\varphi_{\alpha}(\boldsymbol{r}_1)\varphi_{\beta}(\boldsymbol{r}_2)]\rangle, \quad (10)$$

where $\chi^{(-)}$ is the distorted wave function of the outgoing nucleon and $\varphi_{\alpha(\beta)}$ are sp shell-model wave functions.

The current operator can be written as

$$j^{\mu}(\boldsymbol{r},\boldsymbol{r}_1,\boldsymbol{r}_2)=\frac{1}{A-1}[J^{(1)\mu}(\boldsymbol{r},\boldsymbol{r}_1)+J^{(1)\mu}(\boldsymbol{r},\boldsymbol{r}_2)]+J^{(2)\mu}(\boldsymbol{r},\boldsymbol{r}_1,\boldsymbol{r}_2). \quad (11)$$

Therefore, in the model the interaction occurs through one-body and two-body currents with a pair of correlated nucleons. Only one nucleon is emitted and the other nucleon is reabsorbed in the residual nucleus. For the nucleon that is not emitted a sum over all the sp states is included in Eq. (10). The one-body current contains a direct and an exchange term. When the correlation function $f(r_{ij})$ is not included in Eq. (10) only the direct term survives in the one-body current: its contribution corresponds to the DKO mechanism and gives the DWIA result.

In the calculations, the one-body current consists of the usual charge operator and the convective and the spin terms

$$\boldsymbol{J}(\boldsymbol{r},\boldsymbol{r}_k)=\frac{G_E}{2iM}\{\delta(\boldsymbol{r}-\boldsymbol{r}_k),\boldsymbol{\nabla}_k\}-\frac{G_M}{2M}\boldsymbol{\sigma}_k\times\boldsymbol{\nabla}\,\delta(\boldsymbol{r}-\boldsymbol{r}_k), \quad (k=1,2), \quad (12)$$

where the forms factors G_E and G_M are taken from Ref. [31].

The two-body current is derived by performing a nonrelativistic reduction of the lowest-order Feynman diagrams with one-pion exchange. We have thus currents corresponding to the seagull and pion-in-flight diagrams and to the diagrams with intermediate isobar configurations. The contributions included in the calculations are depicted in Fig. 1. Due to current conservation only the transverse components of the two-body current are included.

In the coordinate space, the seagull and pion-in-flight currents are [3]

$$\boldsymbol{J}^{\mathrm{sea}}(\boldsymbol{r},\boldsymbol{r}_1\boldsymbol{\sigma}_1,\boldsymbol{r}_2\boldsymbol{\sigma}_2)=-\frac{f^2}{4\pi}(\boldsymbol{\tau}_1\times\boldsymbol{\tau}_2)_3[\boldsymbol{\sigma}^{(1)}\delta(\boldsymbol{r}_1-\boldsymbol{r})(\boldsymbol{\sigma}^{(2)}\cdot\hat{\boldsymbol{r}}_{12})]\times\left(1+\frac{1}{\mu r_{12}}\right)\frac{e^{-\mu r_{12}}}{\mu r_{12}}+(1\leftrightarrow2), \quad (13)$$

$$\boldsymbol{J}^{\pi}(\boldsymbol{r},\boldsymbol{r}_1\boldsymbol{\sigma}_1,\boldsymbol{r}_2\boldsymbol{\sigma}_2)=-\frac{f^2}{16\pi^2}(\boldsymbol{\tau}_1\times\boldsymbol{\tau}_2)_3\boldsymbol{\nabla}_1(\boldsymbol{\sigma}_1\cdot\boldsymbol{\nabla}_1)\times(\boldsymbol{\sigma}_2\cdot\boldsymbol{\nabla}_2)\frac{e^{-\mu|\boldsymbol{r}_1-\boldsymbol{r}|}}{\mu|\boldsymbol{r}_1-\boldsymbol{r}|}\frac{e^{-\mu|\boldsymbol{r}_2-\boldsymbol{r}|}}{\mu|\boldsymbol{r}_2-\boldsymbol{r}|}+(1\leftrightarrow2), \quad (14)$$

where $f^2/(4\pi)=0.079$ and μ is the pion mass.

The operator form of the Δ current has been derived in Ref. [33]. It is given by the sum of the contributions of two types of processes, corresponding to the Δ-excitation, Figs. 1(d) and 1(e), and Δ-deexcitation currents, Figs. 1(f) and 1(g). The first process (I) describes Δ-excitation by photon absorption and subsequent deexcitation by pion exchange, while the second process (II) describes the time interchange of the two steps, i.e., first excitation of a virtual Δ by pion exchange in a NN collision and subsequent deexcitation by photon absorption. The propagator of the resonance, G_{Δ}, depends on the invariant energy $\sqrt{s}$ of the Δ, which is different for processes I and II. For the deexcitation current the static approximation can be applied, i.e.,

$$G_{\Delta}^{\mathrm{II}}=(M_{\Delta}-M)^{-1}, \quad (15)$$

where $M_\Delta = 1232$ MeV. For the excitation current, we use [34]

$$G_\Delta^{\mathrm{I}} = \left(M_\Delta - \sqrt{s_{\mathrm{I}}} - \frac{\mathrm{i}}{2}\Gamma_\Delta(\sqrt{s_{\mathrm{I}}}) \right)^{-1} \tag{16}$$

with

$$\sqrt{s_{\mathrm{I}}} = \sqrt{s_{NN}} - M, \tag{17}$$

where $\sqrt{s_{NN}}$ is the invariant energy of the two interacting nucleons. The energy-dependent decay width of the Δ, Γ_Δ, has been taken in the calculations according to the parametrization of Ref. [35].

The sum of the two processes gives

$$\begin{aligned} \boldsymbol{J}^\Delta(\boldsymbol{r},\boldsymbol{r}_1\boldsymbol{\sigma}_1,\boldsymbol{r}_2\boldsymbol{\sigma}_2) &= \gamma\delta(\boldsymbol{r}-\boldsymbol{r}_1)\{\mathrm{i}(G_\Delta^{\mathrm{I}}+G_\Delta^{\mathrm{II}})[4\tau_{2,3}\boldsymbol{A}(\boldsymbol{r}_{12},\boldsymbol{\sigma}_1,\boldsymbol{\sigma}_2) \\ &\quad -(\boldsymbol{\tau}_1\times\boldsymbol{\tau}_2)_3\boldsymbol{B}(\boldsymbol{r}_{12},\boldsymbol{\sigma}_1,\boldsymbol{\sigma}_2)]+2(G_\Delta^{\mathrm{I}}-G_\Delta^{\mathrm{II}}) \\ &\quad \times[(\boldsymbol{\tau}_1\times\boldsymbol{\tau}_2)_3\boldsymbol{A}(\boldsymbol{r}_{12},\boldsymbol{\sigma}_1,\boldsymbol{\sigma}_2)+\tau_{2,3}\boldsymbol{B}(\boldsymbol{r}_{12},\boldsymbol{\sigma}_1,\boldsymbol{\sigma}_2)]\} \\ &\quad +(1\leftrightarrow 2), \end{aligned} \tag{18}$$

where

$$\begin{aligned} \boldsymbol{A}(\boldsymbol{r}_{12},\boldsymbol{\sigma}_1,\boldsymbol{\sigma}_2) &= (\boldsymbol{q}\times\hat{\boldsymbol{r}}_{12})(\boldsymbol{\sigma}_2\cdot\hat{\boldsymbol{r}}_{12})Y^{(1)}(r_{12}) \\ &\quad -(\boldsymbol{q}\times\boldsymbol{\sigma}_2)Y^{(2)}(r_{12}), \end{aligned} \tag{19}$$

$$\begin{aligned} \boldsymbol{B}(\boldsymbol{r}_{12},\boldsymbol{\sigma}_1,\boldsymbol{\sigma}_2) &= \boldsymbol{q}\times(\boldsymbol{\sigma}_1\times\hat{\boldsymbol{r}}_{12})(\boldsymbol{\sigma}_2\cdot\hat{\boldsymbol{r}}_{12})Y^{(1)}(r_{12}) \\ &\quad -\boldsymbol{q}\times(\boldsymbol{\sigma}_1\times\boldsymbol{\sigma}_2)Y^{(2)}(r_{12}); \end{aligned} \tag{20}$$

$$Y^{(1)}(r_{12}) = \left(1+\frac{3}{\mu r_{12}}+\frac{3}{\mu^2 r_{12}{}^2}\right)\frac{e^{-\mu r_{12}}}{\mu r_{12}}, \tag{21}$$

$$Y^{(2)}(r_{12}) = \left(\frac{1}{\mu r_{12}}+\frac{1}{\mu^2 r_{12}{}^2}\right)\frac{e^{-\mu r_{12}}}{\mu r_{12}}, \tag{22}$$

and the factor γ collects various coupling constants

$$\gamma = \frac{f_{\gamma N\Delta} f_{\pi NN} f_{\pi N\Delta}}{36\pi\mu}. \tag{23}$$

The operators of the two-body current have been corrected for their behavior at short distances with a hadronic form factor, which was chosen as a monopole function with a cut-off parameter $\Lambda_\pi = 800$ MeV.

III. RESULTS

Calculations have been performed for exclusive $(e,e'p)$ and (γ,p) reactions from ^{16}O. Although the model can in principle be applied to any other target nucleus, we do not expect, on the basis of previous investigations, different effects of two-body currents for different nuclei. The large amount of theoretical and experimental work carried out on ^{16}O, an ample choice of theoretical ingredients available for our calculations, and the possibility of a direct comparison with different sets of data make ^{16}O a well-suited target for our study, which allows us a comparison with our previous calculations and with the results of other and different theoretical models. Moreover, calculations on ^{16}O make it possible to check the consistency of the description of $(e,e'p)$ and (γ,p) reactions in comparison with data.

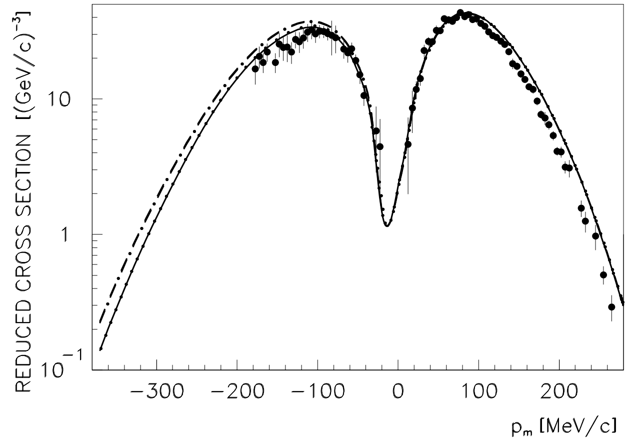

FIG. 2. The reduced cross section of the ^{16}O$(e,e'p)^{15}$N$_{\mathrm{g.s.}}$ reaction as a function of the recoil momentum p_{m} in parallel kinematics, with $E_0 = 520$ MeV and an outgoing proton energy $T_{\mathrm{p}} = 90$ MeV. The data are from Ref. [36]. The optical potential is taken from Ref. [37] and the overlap function is derived from the OBDM of Ref. [14]. The dotted line gives the contribution of the one-body current (DWIA). The other lines have been obtained by adding the various terms of the two-body current: one-body + seagull (dot-dashed lines), one-body + seagull + pion-in-flight (dashed lines), one-body+ seagull+ pion-in-flight+ Δ (solid lines). A reduction factor 0.8 has been applied to the theoretical results. Positive (negative) values of p_{m} refer to situations where $|\boldsymbol{q}|<|\boldsymbol{p}'|$ ($|\boldsymbol{q}|>|\boldsymbol{p}'|$). Dashed and dot-dashed lines are ovelapping in the figure.

A. The ^{16}O$(e,e'p)^{15}$N reaction

A numerical example is shown in Fig. 2 for the ^{16}O$(e,e'p)$ reaction and the transition to the $1/2^-$ ground state of ^{15}N in the parallel kinematics of the experiment carried out at NIKHEF [36]. In parallel kinematics the momentum of the outgoing nucleon $\boldsymbol{p}'$ is fixed and is taken parallel or antiparallel to the momentum transfer $\boldsymbol{q}$. Different values of the recoil momentum $\boldsymbol{p}_{\mathrm{m}}$ are obtained by varying the electron scattering angle and, therefore, the magnitude of the momentum transfer. In order to allow a comparison with data, the results are presented in terms of the reduced cross section [3], which is defined as the cross section divided by a kinematical factor and the elementary off-shell electron-proton scattering cross section, usually taken on the base of the CC1 prescription [38]. Final state interactions are taken into account by the same phenomenological optical potential [37] as in the original DWIA analysis of data [36]. The Coulomb distortion of electron waves is included through the effective momentum approximation [3,5], which is a good approximation for a nucleus as light as ^{16}O.

For the bound state wave function of the emitted proton, we have used the one-nucleon overlap function extracted in Ref. [16] from the asymptotic behavior of the one-body density matrix (OBDM) of Ref. [14], which in the analysis of Ref. [16] was able to give the best and a consistent description of $^{16}\mathrm{O}(e,e'p)^{15}\mathrm{N}$ and $^{16}\mathrm{O}(\gamma,p)^{15}\mathrm{N}$ data. The sp wave functions of the second nucleon in the sum of Eq. (10) are consistently evaluated for all the occupied proton and neutron states.

The overlap function already includes SRC and tensor correlations and a spectroscopic factor 0.9. In order to reproduce the size of the experimental data, a reduction factor 0.8 was applied in Ref. [16] to the calculated reduced cross section. This factor, which is applied also in Fig. 2, can be considered as a further spectroscopic factor to be mostly ascribed to the correlations not included in the OBDM, namely, long-range correlations, which also cause a depletion of the quasihole states. In order to avoid possible double counting, we do not include a correlation function in the two-nucleon wave function of Eq. (10). Thus, the result with the one-body current in Fig. 2 is due only to the direct contribution and in practice corresponds to the DWIA result of Ref. [16]. In any case, no significant effect would be produced by a correlation function in the kinematics here considered for the $(e,e'p)$ reaction.

A different choice of the overlap function would produce a different result, but would not change the role of two-body currents, which is practically negligible in Fig. 2. The seagull current produces a slight enhancement of the reduced cross section calculated with only the one-body current. This enhancement is more visible in the left side of the figure, where higher values of the momentum transfer are involved. No significant effect is obtained when the pion-in-flight term is added, while the Δ-isobar current reduces the calculated cross section and practically cancels the contribution of MEC. This result confirms that a DWIA approach with only a one-body current is able to give a good description of $(e,e'p)$ cross sections.

Another example is presented in Fig. 3, where the cross section of the $^{16}\mathrm{O}(e,e'p)$ reaction is displayed for the transitions to the $1/2^-$ ground state and to the $3/2^-$ excited state of $^{15}\mathrm{N}$ in a kinematics where the energy and momentum transfer are constant, the outgoing proton energy is fixed, and different values of p_{m} are obtained changing the scattering angle of the outgoing proton. Also in this case MEC effects are very small. For the ground state, all the curves practically overlap. For the $3/2^-$ state only a slight reduction of the calculated cross section is produced by the Δ current over the whole distribution.

The effects of the two-body currents on the structure functions f_{11}, f_{01}, and f_{1-1} are shown in Fig. 4 in the same conditions and kinematics as in Fig. 3. The longitudinal component f_{00}, which is not affected by MEC in our model, is not presented in the figure. MEC effects on f_{11} are similar to the results found for the cross section. The seagull term gives a slight enhancement of the one-body result, while the Δ current gives a reduction. The total contribution gives a slight reduction of f_{11} for both transitions. For f_{1-1} a small reduction is obtained for the $1/2^-$ state and negligible effects

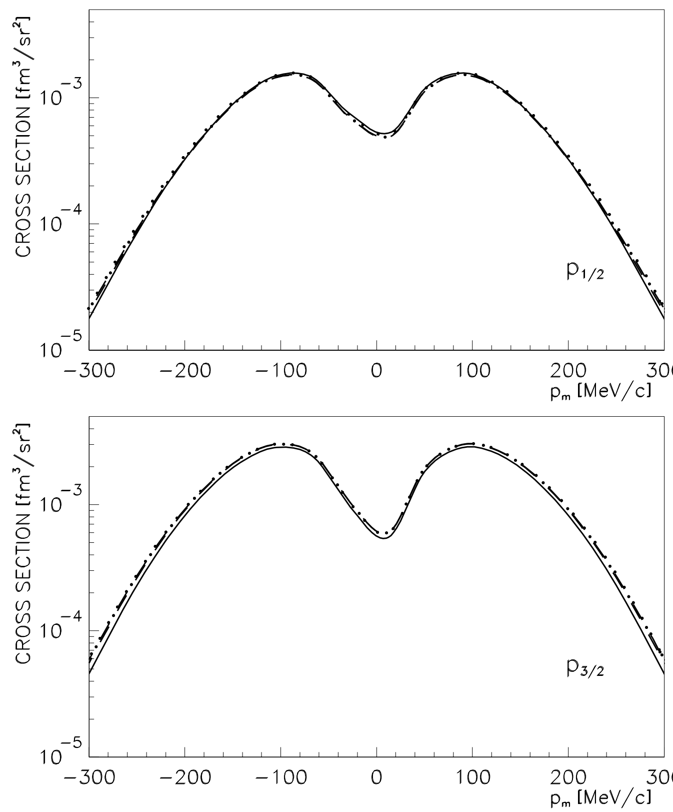

FIG. 3. The cross section of the $^{16}\mathrm{O}(e,e'p)$ reaction as a function of the recoil momentum p_{m} for the transitions to the $1/2^-$ ground state and to the $3/2^-$ excited state of $^{15}\mathrm{N}$ in a kinematics with constant $(\boldsymbol{q},\omega)$, with $E_0 = 2000$ MeV and $T_{\mathrm{p}} = 100$ MeV. The optical potential is taken from Ref. [37]. Overlap functions and line convention as in Fig. 2. Positive (negative) values of p_{m} refer to situations where the angle between $\boldsymbol{p}'$ and the incident electron $\boldsymbol{p}_0$ is larger (smaller) than the angle between $\boldsymbol{q}$ and $\boldsymbol{p}_0$.

for the $3/2^-$ state. This structure function is however very small. The effects of MEC on the interference function f_{01} are different for the two final states. For the ground state, the Δ current cancels the effect produced by the seagull term and makes the contribution of the two-body currents negligible. For the $3/2^-$ state, the seagull and Δ currents contributions sum up in the final result and produce a sizable effect on f_{01}.

A different effect for the two transitions, with a larger contribution of MEC in the $3/2^-$ state, was found also in Ref. [25]. The effects of the isobar currents obtained in our work, however, are much smaller. Our results also differ from those of Ref. [23], where a large contribution was given by the Δ current on f_{11} and f_{1-1} and also on the cross section, but no significant effect was found on f_{01}.

Our results indicate that MEC effects on the exclusive $^{16}\mathrm{O}(e,e'p)^{15}\mathrm{N}$ are in general rather small and of about the same order and relevance as in the analysis of Ref. [27], where, however, no particular difference was found for the structure function f_{01} in the $1/2^-$ and $3/2^-$ states.

Very small MEC effects on the $^{16}\mathrm{O}(e,e'p)^{15}\mathrm{N}$ reaction are found also in the relativistic analysis of Ref. [32], where the calculation of MEC is implemented within the same theoretical framework, but only the seagull term is included in the two-body current.

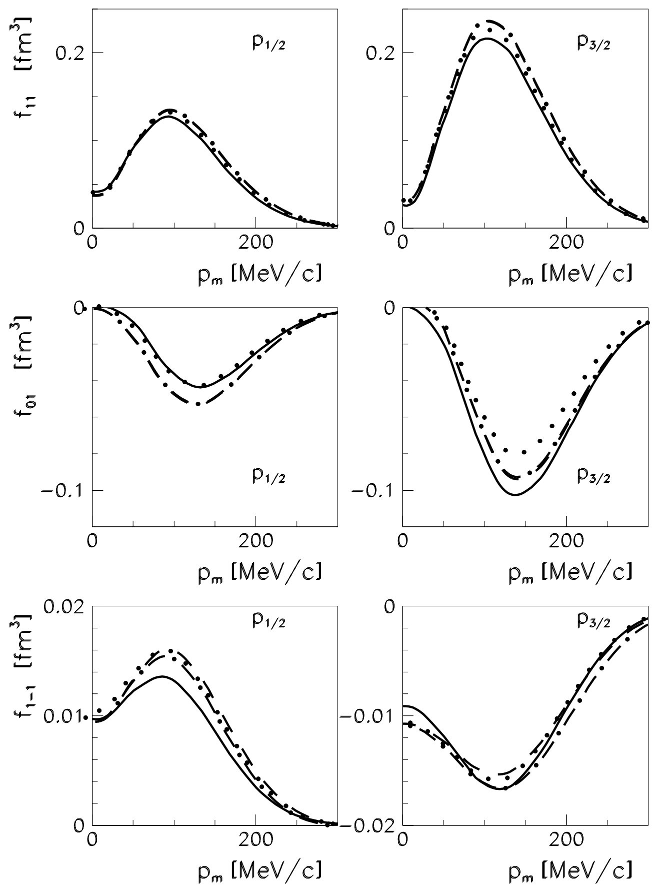

FIG. 4. The structure functions, f_{11}, f_{01}, and f_{1-1}, of the ^{16}O$(e,e'p)$ reaction as a function of the recoil momentum p_{m} for the transitions to the $1/2^-$ ground state and to the $3/2^-$ excited state of ^{15}N in the same kinematics as in Fig. 3. Optical potential, overlap functions, and line convention as in Fig. 3.

B. The ^{16}O$(\gamma,p)^{15}$N reaction

The angular distributions of the ^{16}O(γ,p) reaction at $E_\gamma = 60$ MeV for the transitions to the $1/2^-$ ground state and to the $3/2^-$ excited state of ^{15}N are shown in Fig. 5. In order to check the consistency of $(e,e'p)$ and (γ,p) results in comparison with data and allow a direct comparison with our previous calculations [16], the same theoretical ingredients, i.e., overlap functions and consistent optical potentials, have been adopted as in Ref. [16] and in Fig. 2. Moreover, the reduction factors obtained in comparison with the $(e,e'p)$ data have been applied to the calculated cross sections.

In Fig. 5 the contribution of the one-body current represents a large part of the measured cross section at low scattering angles, but is unable to describe data. A significant enhancement is produced by the seagull current and a reasonable description of data is obtained for the transition to the ground state. This result was already found in Refs. [16,24]: the slight numerical differences are due to the more refined treatment of the spin in the present model, where spin coupling is included and the optical potential contains also the spin-orbit term.

A significant reduction of the cross section is obtained when the pion-in-flight term is added, while the Δ current is

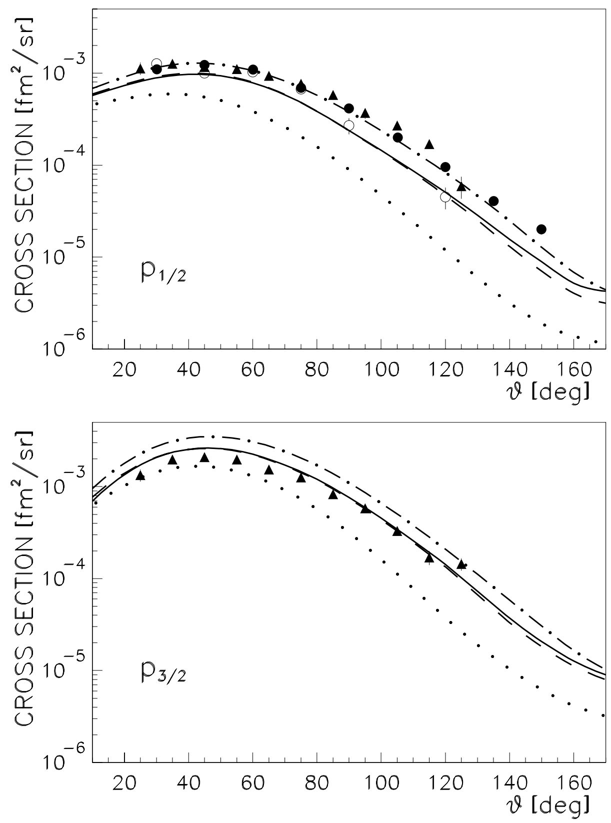

FIG. 5. The cross section of the ^{16}O$(\gamma,p)^{15}$N$_{\mathrm{g.s.}}$ reaction as a function of the proton scattering angle at $E_\gamma = 60$ MeV for the transitions to the $1/2^-$ ground state and to the $3/2^-$ excited state of ^{15}N. The optical potential is taken from Ref. [37] and the overlap functions are derived from the OBDM of Ref. [14]. Line convention as in Fig. 1. The experimental data are taken from Ref. [39] (black circles), Ref. [40] (open circles), and Ref. [41] (triangles). The theoretical results have been multiplied by the reduction factors extracted in Ref. [16] in comparison with $(e,e'p)$ data, that is 0.8 for $1/2^-$ and 0.62 for $3/2^-$ states.

not very important at the considered value of the photon energy. Thus, MEC effects are overestimated by the seagull term, which gives the main contribution of MEC at $E_\gamma = 60$ MeV, but is unable to describe the final effect of two-body currents on the cross section. As a consequence of the reduction produced by the pion-in-flight current, the experimental cross section for the transition to the ground state is somewhat underestimated, while a better agreement with data is found for the $3/2^-$ state. Anyhow, MEC effects remain large and important to improve the agreement with data.

The role of the different terms of the two-body current depends on the photon energy. An example is shown in Fig. 6, where the cross sections of the ^{16}O$(\gamma,p)^{15}$N$_{\mathrm{g.s.}}$ reaction at $E_\gamma = 100$ and 196 MeV are displayed. MEC effects are always large. The role of the seagull current decreases increasing the photon energy. Important effects are given by the pion-in-flight and, at 196 MeV, also by the Δ current. A good agreement with data is achieved at 100 MeV when the pion-in-flight term is added. Here pion-in-flight reduces the contribution given by seagull for nucleon emission angles up to

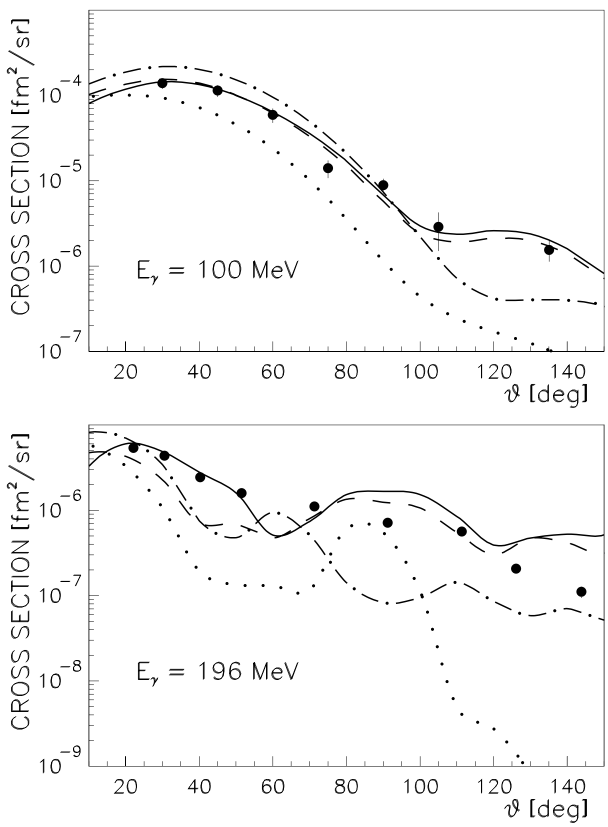

FIG. 6. The cross sections of the $^{16}O(\gamma,p)^{15}N$ reaction as a function of the proton scattering angle at $E_\gamma = 100$ and 196 MeV. Overlap function and line convention as in Fig. 4. The optical potential is taken from Ref. [37]. The experimental data are taken from Refs. [39] ($E_\gamma = 100$) and [42] ($E_\gamma = 196$). The theoretical results have been multiplied by the reduction factor 0.8 as in Figs. 1 and 4.

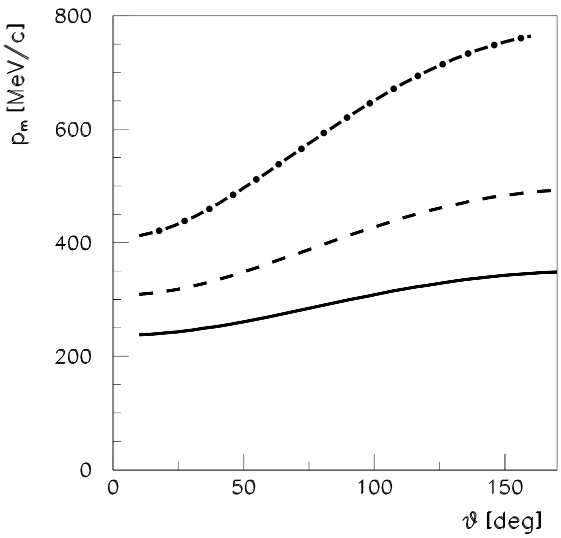

FIG. 7. The recoil momentum p_m as a function of the proton scattering angle for the $^{16}O(\gamma,p)^{15}N$ reaction at $E_\gamma = 60$ (solid line), 100 (dashed line), and 196 MeV (dot-dashed line).

$\sim 100^o$, while at larger angles it produces a significant enhancement of the cross section. At 196 MeV a good agreement with data is obtained for nucleon emission angles up to $\sim 70°$ when the Δ current is added, while for larger angles the strong enhancement produced mainly by the pion-in-flight term leads to some overestimation of the experimental cross section. In this region, however, recoil-momentum values around 700–800 MeV/c are probed (see Fig. 7), where the behavior of the wave function may become critical and other effects might come into play. Moreover, the convergence of the integrals in the calculation of the matrix elements of the two-body current becomes slow.

Our results indicate that two-body currents give an important contribution to (γ,p) cross sections at all the considered photon energies. When all the one-pion-exchange diagrams are included in the model, a reasonable description of $(e,e'p)$ data, for recoil momentum values up to ~ 300 MeV/c, and of (γ,p) data, at least up to ~ 500–600 MeV/c, is obtained, with a consistent choice of the theoretical ingredients and with the same spectroscopic factors.

The effect of SRC is investigated in Fig. 8 for the $^{16}O(\gamma,p)^{15}N_{g.s.}$ reaction at $E_\gamma = 60$ and 196 MeV. All the cross sections have been calculated with the phenomenological sp bound state wave functions of Ref. [43], which do not include correlations. The results shown in the left panels have been obtained without a correlation function, while the cross sections in the right panels include the correlation function of Ref. [44], extracted form a recent application of Green's function techniques to the calculation of relative two-nucleon wave functions in nuclear matter. Correlation effects are small at 60 MeV, where they produce only a slight enhancement of the cross section that anyhow improves the agreement with data. At 196 MeV SRC produce a strong enhancement of the contribution of the one-body current for nucleon emission angles above 70°, in the region where high values of the recoil momentum are probed and the cross section is dominated by two-body currents. An opposite effect is given by the correlation function on the two-body current. The contributions of the Δ and seagull currents are significantly reduced by SRC at large angles, while correlation effects are not very important on the pion-in-flight term. In the final result, the effect of SRC is overwhelmed by the contribution of two-body currents, as it was found also in Ref. [29]. The effect of SRC is anyhow non-negligible and improves the agreement with data.

The behavior of the separate contributions of the different terms of the nuclear current is also shown in Fig. 8. At $E_\gamma = 60$ MeV the one-body current gives a large part of the final result and is already able to correctly reproduce the shape of the angular distribution. The seagull current is also important, in particular at large scattering angles. The sum of the two terms produces, as in Fig. 5, a significant enhancement of the cross section. The pure contribution of pion-in-flight is much smaller than those of the one-body and seagull currents, but it produces a strong destructive interference with seagull. The Δ current gives only a negligible contribution. At 196 MeV the one-body current gives only a small fraction of the experimental cross section. The final result is dominated by two-body currents, mainly by the isobar current at small proton emission angles and by the pion-in-flight term

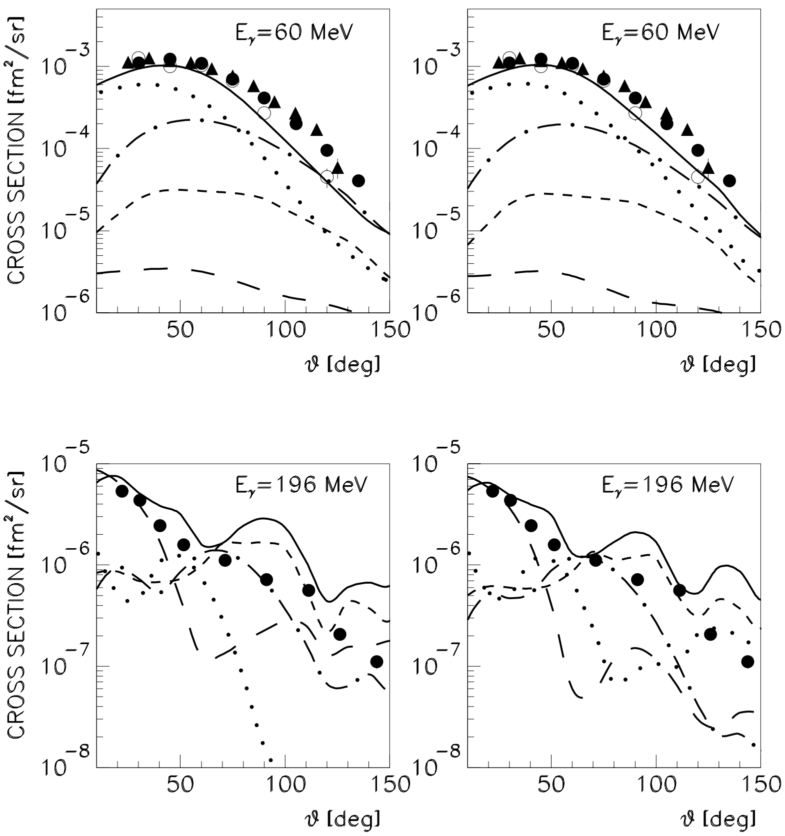

FIG. 8. The cross sections of the ^{16}O(γ,p)^{15}N$_{\text{g.s.}}$ reaction as a function of the proton scattering angle at E_γ=60 and 196 MeV. Optical potential and experimental data as in Figs. 5 and 6. The bound state wave functions are taken from Ref. [43]. The theoretical results shown in the right panels have been obtained including in the two-nucleon wave function the correlation function of Ref. [44]. Line convention for dotted and solid lines as in Fig. 1. The dot-dashed, long-dashed, and short-dashed lines give the pure contributions of the seagull, Δ, and pion-in-flight currents, respectively. The theoretical results have been multiplied by the reduction factor 0.8, consistently with the analysis of $(e,e'p)$ data for the same bound state wave function.

at large angles. The seagull current is not very important. At high values of the recoil momentum sizable and different contributions are given by SRC on the various components of the current. However, the combined effect does not appear large in the final result and is overwhelmed by MEC.

Our results for the (γ,p) reactions are qualitatively similar to the results found in Ref. [29]. The quantitative numerical differences are compatible with the different theoretical ingredients used in the two calculations, as the (γ,p) cross sections are very sensitive to details of the model. A different choice of these ingredients might change the numerical results, but should not change the main conclusions of our work.

IV. SUMMARY AND CONCLUSIONS

The role of MEC in exclusive $(e,e'p)$ and (γ,p) reactions has been studied in the frame of a nonrelativistic DKO model with final state interactions. The nuclear current is the sum of a one-body part, including the convective and the spin terms, and of a two-body part, including the contribution of all the diagrams with one-pion exchange, namely, seagull, pion-in-flight and the diagrams with intermediate Δ-isobar configurations. The direct contribution of the one-body current corresponds to the DKO mechanism and gives the DWIA. Final state interactions are treated with a phenomenological and spin dependent optical potential. Correlations can be included in the sp wave functions or with a central correlation function.

Numerical results have been presented in different kinematics for electron- and photon-induced reactions from ^{16}O, in order to allow a comparison with previous calculation and to check the consistency of the description of the two reactions also in comparison with data.

The role of two-body currents on the ^{16}O$(e,e'p)^{15}$N cross section is in general rather small. This result confirms once more the validity of the DWIA approach for this reaction. MEC give in general a small contribution also on the structure functions. The effects are of about the same order and relevance as in the analysis of Ref. [27], but a different behavior is found in our model on the interference longitudinal-transverse structure function f_{01} for the transitions to the $1/2^-$ ground state and to first $3/2^-$ excited state of ^{15}N. For the $1/2^-$ state, the Δ current cancels the effect produced by the seagull term and the contribution of MEC is negligible. For the $3/2^-$ state, the contributions of the two terms sum up and produce a sizable effect in the final result. A different behavior on f_{01} for the two states was found also in Ref. [25], where, however, the contribution of MEC, and in particular of the Δ current, is much larger than in our model.

Results have been presented for the ^{16}O$(\gamma,p)^{15}$N cross section at E_γ=60, 100, and 196 MeV. At all the considered photon energies MEC give an important contribution which substantially improves the agreement with data. At E_γ =60 MeV the DKO mechanism represents a large part of the experimental cross section, but underestimates the size of the data. The role of the one-body current on the cross section becomes less important increasing the photon energy and the proton emission angle. A significant enhancement is produced by the seagull current. At 60 MeV the seagull term gives the main contribution of the two-body currents, but overestimates their final effect. A strong destructive interference is obtained when the pion-in-flight term is added. The contribution of the seagull current decreases increasing the photon energy. Important contributions are given at higher energies by the pion-in-flight, in particular at large angles, and at 196 MeV also by the Δ current.

Significant and different effects on the various terms of the nuclear current are given by SRC at high values of the recoil momentum. The combined effect, however, does not appear large in the final result and is in general overwhelmed by MEC.

When all the one-pion exchange diagrams are included in the model, calculations with consistent theoretical ingredients, i.e., bound state wave functions, optical potentials, and the same spectroscopic factors, are able to give a reasonable and consistent description of the experimental cross sections of the $^{16}\mathrm{O}(e,e'p)^{15}\mathrm{N}$ knockout for recoil momenta up to ~ 300 MeV/c and of the $^{16}\mathrm{O}(\gamma,p)^{15}\mathrm{N}$ reaction up to ~ 500–600 MeV/c. For higher momentum values, other effects might come into play and also a more careful treatment of correlations would presumably deserve further investigation.

ACKNOWLEDGMENTS

We thank A. N. Antonov and M. K. Gaidarov for providing us the overlap functions used in the calculations and G. Co' for useful discussions.

[1] S. Frullani and J. Mougey, Adv. Nucl. Phys. **14**, 1 (1984).

[2] S. Boffi, C. Giusti, and F.D. Pacati, Phys. Rep. **226**, 1 (1993).

[3] S. Boffi, C. Giusti, F.D. Pacati, and M. Radici, *Electromagnetic Response of Atomic Nuclei*, Oxford Studies in Nuclear Physics, Vol. 20 (Clarendon, Oxford, 1996).

[4] J.J. Kelly, Adv. Nucl. Phys. **23**, 75 (1996).

[5] C. Giusti and F.D. Pacati, Nucl. Phys. **A473**, 717 (1987); **A485**, 461 (1988).

[6] Y. Jin, D.S. Onley, and L.E. Wright, Phys. Rev. C **45**, 1311 (1992); Y. Jin, J.K. Zhang, D.S. Onley, and L.E. Wright, *ibid.* **47**, 2024 (1993); Y. Jin and D.S. Onley, *ibid.* **50**, 377 (1994).

[7] J.M. Udías, P. Sarriguren, E. Moya de Guerra, E. Garrido, and J.A. Caballero, Phys. Rev. C **48**, 2731 (1993); **51**, 3246 (1995); J.M. Udías, P. Sarriguren, E. Moya de Guerra, and J.A. Caballero, Phys. Rev. C **53**, R1488 (1996); J.M. Udías, J.A. Caballero, E. Moya de Guerra, J.E. Amaro, and T.W. Donnelly, Phys. Rev. Lett. **83**, 5451 (1999).

[8] J.M. Udías and J.R. Vignote, Phys. Rev. C **62**, 034302 (2000).

[9] A. Meucci, C. Giusti, and F.D. Pacati, Phys. Rev. C **64**, 014604 (2001); **64**, 064615 (2001).

[10] J. Gao *et al.*, Phys. Rev. Lett. **84**, 3265 (2000).

[11] A. Fabrocini and G. Co', Phys. Rev. C **63**, 044319 (2001).

[12] S.R. Mokhtar, M. Anguiano, G. Co', and A.M. Lallena, Ann. Phys. (N.Y.) **293**, 67 (2001).

[13] D. Van Neck, L. Van Daele, Y. Dewulf, and M. Waroquier, Phys. Rev. C **56**, 1398 (1997).

[14] A. Polls, H. Müther, and W.H. Dickhoff, in *Proceedings of the Conference on Perspectives in Nuclear Physics at Intermediate Energies, Trieste, 1995*, edited by S. Boffi, C. Ciofi degli Atti, and M.M. Giannini (World Scientific, Singapore, 1996), p. 308.

[15] A. Polls, M. Radici, S. Boffi, W.H. Dickhoff, and H. Müther, Phys. Rev. C **55**, 810 (1997).

[16] M.K. Gaidarov, K.A. Pavlova, A.N. Antonov, M.V. Stoitsov, S.S. Dimitrova, M.V. Ivanov, and C. Giusti, Phys. Rev. C **61**, 014306 (2000).

[17] M. Anguiano and G. Co', J. Phys. G **27**, 2109 (2001).

[18] W.J.W. Geurts, K. Allaart, W.H. Dickhoff, and H. Müther, Phys. Rev. C **53**, 2207 (1996).

[19] K. Amir-Azimi-Nili, H. Müther, L.D. Skouras, and A. Polls, Nucl. Phys. **A604**, 245 (1996); K. Amir-Azimi-Nili, J.M. Udías, H. Müther, L.D. Skouras, and A. Polls, *ibid.* **A625**, 633 (1997).

[20] C. Barbieri and W. H Dickhoff, Phys. Rev. C **63**, 034313 (2001); **65**, 064313 (2002).

[21] P. Demetriou, S. Boffi, C. Giusti, and F.D. Pacati, Nucl. Phys. **A624**, 513 (1997); **A634**, 57 (1998); P. Demetriou, A. Gil, S. Boffi, C. Giusti, E. Oset, and F.D. Pacati, *ibid.* **A650**, 199 (1999).

[22] P.K.A. de Witt Huberts, J. Phys. G **16**, 507 (1990); L. Lapikás, Nucl. Phys. **A553**, 297c (1993).

[23] S. Boffi and M. Radici, Phys. Lett. B **242**, 151 (1990); S. Boffi, C. Giusti, F.D. Pacati, and M. Radici, Nucl. Phys. **A518**, 639 (1990); S. Boffi and M. Radici, *ibid.* **A526**, 602 (1991); S. Boffi, M. Radici, J.J. Kelly, and T.M. Payerle, *ibid.* **A539**, 597 (1992).

[24] G. Benenti, C. Giusti, and F.D. Pacati, Nucl. Phys. **A574**, 716 (1994).

[25] V. Van der Sluys, J. Ryckebusch, and M. Waroquier, Phys. Rev. C **49**, 2695 (1994); **54**, 1322 (1996).

[26] J. Ryckebusch, D. Debruyne, W. Van Nespen, and S. Janssen, Phys. Rev. C **60**, 034604 (1999).

[27] J.E. Amaro, A.M. Lallena, and J.A. Caballero, Phys. Rev. C **60**, 014602 (1999).

[28] J. Ryckebusch, Phys. Rev. C **64**, 044606 (2001).

[29] M. Anguiano, G. Co', A.M. Lallena, and S.R. Mokhtar, Ann. Phys. (N.Y.) **296**, 235 (2002).

[30] M.V. Ivanov, M.K. Gaidarov, A.N. Antonov, and C. Giusti, Phys. Rev. C **64**, 014605 (2001).

[31] G.G. Simon, Ch. Schmitt, F. Borkowski, and V.H. Walther, Nucl. Phys. **A333**, 381 (1980).

[32] A. Meucci, C. Giusti, and F.D. Pacati, Phys. Rev. C **66**, 034610 (2002).

[33] P. Wilhelm, H. Arenhövel, C. Giusti, and F.D. Pacati, Z. Phys. A **359**, 467 (1997).

[34] Th. Wilbois, P. Wilhelm, and H. Arenhövel, Phys. Rev. C **54**, 3311 (1996).

[35] B.H. Bransden and R.G. Moorhouse, *The Pion-Nucleon System* (Princeton University Press, Princeton, 1973).

[36] M. Leuschner, J.R. Calarco, F.W. Hersman, E. Jans, G.J.

Kramer, L. Lapikás, G. van der Steenhoven, P.K.A. de Witt Huberts, H.P. Blok, N. Kalantar-Nayestanaki, and J. Friedrich, Phys. Rev. C **49**, 955 (1994).

[37] P. Schwandt, H.O. Meyer, W.W. Jacobs, A.D. Bacher, S.E. Vigdor, M.D. Kaitchuck, and T.R. Donoghue, Phys. Rev. C **26**, 55 (1982).

[38] T. de Forest, Jr., Nucl. Phys. **A392**, 232 (1983).

[39] D.J.S. Findlay and R.O. Owens, Nucl. Phys. **A279**, 389 (1977).

[40] F. de Smet, H. Ferdinande, R. Van de Vyver, L. Van Hoorebeke, D. Ryckbosch, C. Van den Abeele, J. Dias, and J. Ryckebusch, Phys. Rev. C **47**, 652 (1993).

[41] G.J. Miller, J.C. McGeorge, J.R.M. Annand, G.I. Crawford, V. Holliday, I.J.D. MacGregor, R.O. Owens, J. Ryckebusch, J.-O. Adler, B.-E. Andersson, L. Isaksson, and B. Schröder, Nucl. Phys. **A586**, 125 (1995).

[42] G.S. Adams, E.R. Kinney, J.L. Matthews, W.W. Sapp, T. Soos, R.O. Owens, R.S. Turley, and G. Pignault, Phys. Rev. C **38**, 2771 (1988).

[43] L.R.B. Elton and A. Swift, Nucl. Phys. **A94**, 52 (1967).

[44] C.C. Gearhart, Ph.D. thesis, Washington University, St. Louis, 1994; C.C. Gearhart and W.H. Dickhoff (private communication).